

1 **Effects of Direct Injection Timing Associated with Spark Timing on a Small Spark**
2 **Ignition Engine Equipped with Ethanol Dual-Injection**

3 Nizar F.O. Al-Muhsen¹, Yuhan Huang², Guang Hong¹

4

5 ¹School of Mechanical and Mechatronic Engineering, University of Technology Sydney,
6 Sydney, Australia

7 ²School of Civil and Environmental Engineering, University of Technology Sydney, Sydney,
8 Australia

9

10 Corresponding author:

11 Nizar F.O. Al-Muhsen, Ph.D. student

12 Postal address: School of Mechanical and Mechatronic Engineering, Faculty of Engineering
13 & IT, University of Technology Sydney, PO Box 123, Broadway NSW 2007, Australia

14 Emails: Nizar.Al-Muhsen@student.uts.edu.au

15 Telephone: +61 426098211

16

17 **Abstract**

18 Dual injection of ethanol fuel (DualEI) has been in development. DualEI has the potential in
19 increasing the compression ratio and thermal efficiency of spark ignition engines by taking
20 the advantages of ethanol fuel properties and the direct injection. This paper reports an
21 experimental investigation of the effect of direct injection (DI) timing associated with spark
22 timing on the performance of a small DualEI engine. Experiments were conducted with fixed
23 port injection timing and varied DI timing before (early) and after (late) the intake valve
24 closed at 3500 RPM and two load conditions. Results show that the engine performance is
25 enhanced by early DI timing, although the variation of IMEP and indicated thermal efficiency
26 with DI timing is not significant either with early DI timing or in most of the tested
27 conditions with late DI timing. Only in the medium load condition when the DI timing is
28 retarded from 80 to 60 CAD bTDC, the IMEP and thermal efficiency significantly reduced
29 by about 16% due to the increased initial combustion duration, resulting in reduced flame
30 speed and increased combustion instability. The results also show different effects of early
31 and late DI timing associated with the spark timing on engine emissions. With late DI timing,
32 the engine emissions of CO and NO increase with the advance of late DI timing and spark
33 timing. With early DI timing, the engine emissions increase with the advance of spark timing.
34 However, the variation of engine emissions with early DI timing is more complicated than
35 that late.

36 **Keywords**

37 Ethanol dual-injection (DualEI); Ethanol direct injection; Injection timing; Spark timing;
38 Combustion; Emissions

39

40 **Highlights**

- 41 ➤ Effect of DI timing was stronger than the spark timing on DualEI engine performance.
- 42 ➤ IMEP and indicated thermal efficiency were improved with early DI timing compared to
43 that of late DI timing.
- 44 ➤ ISCO was decreased when DI timing was advanced from late to early DI timing.
- 45 ➤ ISNO was decreased by enhanced charge cooling effect when DI timing was retarded
46 from early to late DI timing.

47 **Abbreviations**

bTDC	before top dead centre
CAD	crank angle degree
CA10-90%	the major combustion duration
CA0-10%	the minor combustion duration
CA50	combustion phase when 50% of the fuel is burnt.
DI	direct injection
DIT	direct injection timing
DualEI	ethanol dual-injection
EDI+GPI	ethanol direct injection plus Gasoline port injection
EPI	ethanol port injection
GDI	gasoline direct injection
HRR _{max}	maximum heat release rate
IMEP	indicated mean effective pressure
ISCO	indicated specific carbon monoxide
ISFC	indicated specific fuel consumption
ISHC	indicated specific hydrocarbon
ISNO	indicated specific nitric oxide
MBT	minimum spark advance for best torque
P _{max}	maximum cylinder pressure
ST	spark timing
λ	air/fuel equivalent ratio

48 **1 Introduction**

49 Replacing fossil fuel by renewable or alternative fuels has been driven by the concerns of
50 sustainability and environmental protection. Moreover, the ever increasingly tightened
51 legislations are enforced to reduce emissions produced by internal combustion (IC) engines.
52 Compared to Euro 3, Euro 6 lowered the nitric oxide (NO), carbon monoxide (CO) and
53 hydrocarbon (HC) emission limits by 60%, 57% and 50% for light-duty cars respectively [1].
54 These legislations highlighted the significance of environmental protection. Ethanol fuel has
55 been used widely as an alternative fuel in IC engines to address the issue of sustainability [2].
56 Ethanol is a renewable fuel produced from a variety of bio-resources. Compared to gasoline,
57 ethanol has a greater flame speed, octane number, and heat of vaporisation, leading to
58 potentially cleaner combustion [3]. Furthermore, the lower adiabatic flame temperature and
59 greater cooling effect could result in a lower combustion temperature and thus less
60 convective heat losses [4]. Nevertheless, ethanol has a lower heating value, which
61 consequently increases the fuel consumption compared to gasoline. The slow evaporation rate
62 of ethanol fuel is also reported at low ambient temperature [5].

63 Injecting fuel directly into the combustion chamber is an approach to improve the engine
64 performance and reduce the pollutant emissions in gasoline engines. The market of vehicles
65 equipped with gasoline direct injection (GDI) engines is continuously increasing globally [6].
66 However, GDI comes with some drawbacks such as particular matter (PM) and greater
67 hydrocarbon (HC) emissions due to fuel impingement [7]. Therefore, it is important to
68 understand the effect of operating parameters on combustion in a GDI engine, such as direct
69 injection (DI) timing and spark timing. Wang et al. [8] investigated the effect of injection
70 strategy on PM emissions in a GDI engine fuelled with ethanol or gasoline. It was found that
71 using high DI pressure and ethanol fuel could potentially reduce the PM emissions, due to the

72 finer droplets and less fuel impingement of higher injection pressure, and greater combustion
73 speed and oxygen content of ethanol fuel.

74 Blended fuels (e.g., ethanol-gasoline and ethanol-diesel blends) were extensively studied in
75 engine research [9, 10]. Bielaczyc et al. [10] tested a spark ignition (SI) engine under a wide
76 range of ethanol-gasoline blending ratios from 5% to 85%. Their results showed that the
77 combustion performance was enhanced due to the greater combustion speed and the oxygen
78 component of ethanol fuel. The higher auto-ignition temperature, the greater latent heat of
79 vaporisation and the larger research octane number of ethanol fuel could mitigate the engine
80 knock. Greater ethanol percentages were commonly used in Brazil and the United States
81 aiming to reduce the dependence on fossil fuels and improve the engine performance [11,
82 12]. The effect of E85 (15% gasoline plus 85% ethanol) on the SI engine performance was
83 investigated [13-16]. Although ethanol is renewable, adopting ethanol as an alternative fuel to
84 gasoline can come with challenges [17]. The lower vapor pressure and heating value of
85 ethanol are two challenges for SI engines [18]. As a result, flex-fuel systems have been used
86 as an auxiliary system to help SI engine in cold starting by using gasoline fuel [19]. Nakata et
87 al. and Taniguchi et al. [20, 21] investigated the feasibility of running the SI engine with
88 ethanol fuel only and concluded that ethanol could improve the engine thermal efficiency. It
89 was reported that 100% ethanol direct injection (EDI) could improve the engine performance
90 and reduce the NO emission [11, 22]. However, the over-cooling effect and severe fuel
91 impingement of pure EDI were represented as possible issues to the SI engines [23].

92 Zhuang et al. [24, 25] investigated the effects of EDI on a gasoline port injection (GPI)
93 engine. It was reported that the combustion performance was significantly improved when
94 EDI was used. Huang et al. analysed the combustion process numerically of the same engine
95 [5, 23]. Their results showed that the engine performance was improved when EDI ratio was
96 within 60%. However, further increase of EDI ratio could deteriorate the combustion quality

97 due to the ethanol impingement and over-cooling effect. The greater laminar flame speed and
98 the oxygen content of ethanol enhanced the combustion performance. A significant reduction
99 of NO emission occurred due to the lower adiabatic flame temperature of ethanol and the
100 cooling effect of EDI strategy. However, HC and CO emissions increased considerably due
101 to the rich mixture regions created inside the combustion chamber when EDI was used. These
102 ethanol rich regions were attributed to ethanol film formed on the combustion chamber walls.
103 Zhu et al. [26] tested the effect of different ethanol-gasoline dual-injection strategies on the
104 combustion characteristics, including GPI plus GDI, GPI plus EDI and ethanol port injection
105 (EPI) plus GDI. The best combustion performance was recorded for GPI+EDI, in which the
106 indicated mean effective pressure (IMEP) increased by 2% at light load.

107 Optimising the combustion phase is a vital method that could potentially improve the engine
108 performance [27]. CA50 defines the crank angle degree (CAD) at which 50% of the mass
109 fuel is burnt [28, 29]. The effect of CA50 on the SI engine performance was extensively
110 investigated [28-31]. The cylinder volume at the position of CA50 and heat released rate
111 (HRR) are factors that can significantly influence the engine performance. Ayala et al.
112 examined the correlation between CA50 and IMEP at a range of equivalence and
113 compression ratios [29]. Their results showed the importance of CA50 to the peak in-cylinder
114 pressure (P_{max}) and its phase (Θ_{Pmax}). It is well known that retarding or advancing the spark
115 timing (ST) from the optimal position of CA50 reduces the engine power [32, 33]. This is
116 caused by the P_{max} reduction and the shift of Θ_{Pmax} from the optimal phase.

117 Controlling the DI timing is another approach to optimise the combustion phase and improve
118 the engine performance. The significance of DI timing comes from its effect on the quality of
119 the mixture. Advanced DI timing gives the fuel more time to atomise, evaporate and mix with
120 air. However, fuel impingement could increase due to the smaller combustion chamber and
121 lower cylinder pressure, resulting in higher HC emission [24]. Retarding DI timing could

122 reduce fuel film, but reduces the time available for air-fuel mixing as well. Davy et al. [34]
123 experimentally investigated the effect of DI timing on the fuel spray development inside a
124 GDI prototype engine. They found that the fuel impingement, especially to the piston surface,
125 reduced significantly due to larger cylinder volume at the retarded DI timing. This might
126 enhance combustion efficiency and reduce the HC and CO emissions simultaneously.
127 However, the NO emission could increase due to greater combustion temperature caused by
128 higher HRR [3].

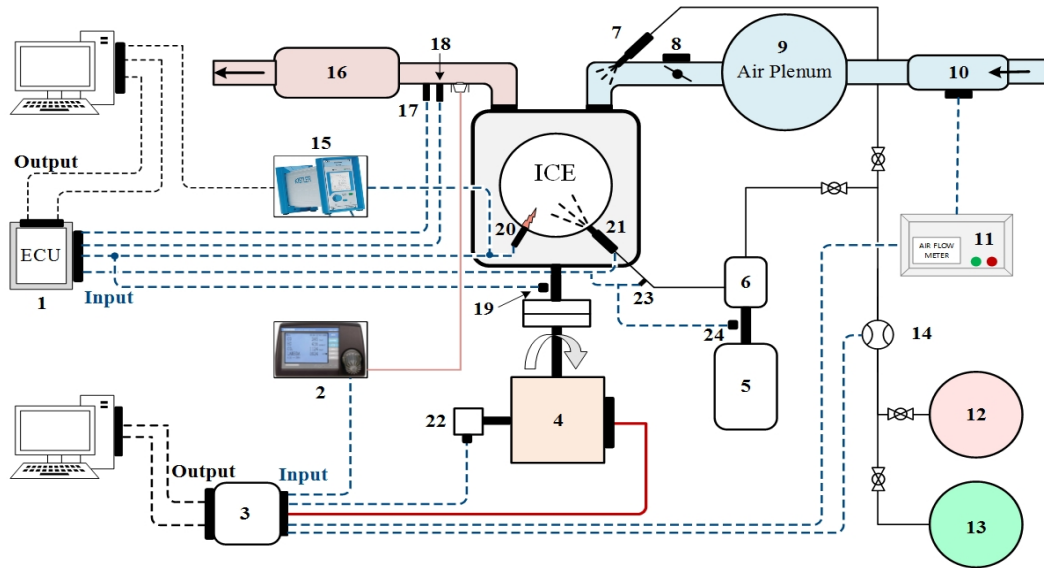
129 As discussed above, adopting ethanol fuel in SI engine development could present new
130 challenges. Different technologies were used to exploit the benefits of ethanol, although the
131 fossil fuel like gasoline is still the main fuel for SI engines. In this paper, a DualEI (EDI plus
132 EPI) was used to provide a better method to fully utilize the properties of ethanol fuel in
133 improving the performance of SI engines. Experiments were conducted to investigate the
134 effect of DI timing associated with spark timing on the DualEI engine performance. The
135 relevant results of the combustion and emissions characteristics were presented and analysed.

136 **2 Experimental Apparatus and Procedure**

137 **2.1 Engine Setup**

138 The experiments were performed on a modified Yamaha YBR250 motorcycle engine as
139 shown in Figure 1. The YBR250 engine is a single cylinder four-stroke air-cooled naturally
140 aspirated SI engine. This engine was chosen because it offers the flexibility for engine
141 modification and is suitable for engine downsizing research. Table 1 shows the major
142 specifications of the engine. The engine was originally equipped with a GPI system. It was
143 modified to be equipped with a DualEI system by Hents Technology to meet the research
144 needs. The engine modification included the installation of a DI system and an electronic
145 control unit (ECU). The ECU was used to control simultaneously the throttle position, spark

146 timing, DI timing and pressure, and DI and PI durations. The DI system comprised of a
147 returnless high-pressure pump and a six-hole high-pressure injector [35]. The injector was
148 side mounted between the intake valve seat and the spark plug [25]. The slope angles of the
149 injector are 15° from the horizontal surface of the cylinder head to the axis of the injector and
150 12° from the vertical surface of the cylinder head. Table 2 shows the major specifications of
151 the injector. More details about the spray plume bend angles and their distribution can be
152 found in [18]. A super-micro LSN39 fuel flow meter with ±3% accuracy was used to measure
153 ethanol flow rates of PI and DI. An eddy current dynamometer was used to control the engine
154 speed and measure the torque. A Kistler 6115B spark plug pressure transducer and a Kistler
155 5011 charge amplifier were used to measure the in-cylinder pressure. K-type thermocouples
156 were used to measure the cylinder head temperature and exhaust gas temperature with a
157 resolution of 0.1 °C and uncertainty of 0.35%. A MEXA-584L Horiba exhaust gas analyser
158 was used to measure the exhaust gas emissions of CO, CO₂, HC and NO, and to calculate the
159 equivalence ratio (λ). The H/C and O/C ratios were manually set in the gas analyser to be 3.0
160 and 0.5 respectively. The intake airflow was stabilised in an 80L intake buffer tank and
161 measured using a ToCeIL20N thermal air-mass flow meter.



1. Electronic Control Unit (ECU) 2. Horiba MXEA-584L Exhaust Gas Analyser 3. NI-Module and Dynamometer Controller 4. Eddy Current Dynamometer 5. Electrical Motor 6. High Pressure Fuel Pump 7. Low Pressure Fuel Injector 8. Step Motor and Throttle Valve Position Sensor 9. Intake Air Stabiliser (Air Plenum) 10. Intake Air Flow Sensor 11. TOCEIL Air Flow Meter 12. Unleaded Gasoline Tank 13. Pure Ethanol Tank 14. Super Micro M-39 Fuel Flow Meter 15. KISTLER-5015A Charge Amplifier 16. Exhaust Gas Catalyser 17. K-Type Thermocouple 18. Bosh Wide-Band Lambda Sensor 19. Crank Shaft Encoder 20. KISTLER-6115B Spark Plug Pressure Transducer 21. High Pressure Fuel Injector 22. S-Type Load Cell 23. Common Rail High Pressure Sensor 24. High Pressure Fuel System Encoder

162
163
164

Figure 1. Ethanol dual-Injection research engine.

Table 1. Specifications of the ethanol dual-injection research engine

Engine Type	Single cylinder, four-stroke, air-cooled, naturally aspirated, SI
Displacement	249.0 cc
Bore	74.0 mm
Stroke	58.0 mm
Compression Ratio	9.8:1
Intake Valve Open (IVO)	382.2 CAD bTDC
Intake Valve Close (IVC)	126.2 CAD bTDC
Exhaust Valve Open (EVO)	594.6 CAD bTDC
Exhaust Valve Close (EVC)	340.7 CAD bTDC

165

Table 2. Specifications of the direct fuel injector [18, 36]

Manufacturer	Bosch
Operating pressure	Up to 500 bar
Number of holes	6 holes
Hole diameter	110 μm
Flow rate @ 100 bar	Up to 1640 g/min
Spray angle single beam	17°
Operating temperature range	-31 to 130 °C

166 2.2 Experimental Procedure

167 The engine was started and warmed up using GPI until the cylinder head temperature became
168 stable at around 200 °C. Then GPI was switched to EPI and the air/fuel ratio was kept at
169 stoichiometric point. Table 3 shows the tested engine conditions. The volumetric ratio (DI%)
170 of the ethanol DI to PI was kept at 50% at light load and 56% at medium load because they
171 were the optimal DI ratios for achieving effective cooling with minimal fuel impingement
172 [23]. The fuel heating value was fixed at around 420 J/cycle at light load and 610 J/cycle at
173 medium load. The spark timing was swept from 19 to 25 CAD bTDC (denoted by ST'XX'
174 hereafter) at light load and from ST28 to ST34 at medium load, as they were the spark
175 timings to produce the maximum output power [37]. At each spark timing, DI timing was
176 varied from 330 CAD bTDC to 240 CAD bTDC (denoted by DIT'XXX' hereafter) before the
177 intake valve was closed (early DI timing), and from DIT120 to DIT60 after the intake valve
178 closed (late DI timing). The range of the late DI timing was chosen to eliminate the effect of
179 the hot residuals, hot combustion chamber walls and intake flow velocity and then to address
180 the effect of DI timing more independently. The range of early DI timing was chosen to
181 include the impact of the previously mentioned factors and the time on engine performance.
182 As shown in Figure 2, the early injection was swept with 30 CAD increment, and the late
183 injection was swept with 20 CAD increment. The DI timing between DIT240 and DIT120
184 was avoided due to the pressure fluctuation when the intake valve was closing [24]. The
185 throttle position was set at 23% for light load and 34% for a medium load. The air/fuel
186 equivalence ratio (λ) was kept at around the stoichiometric condition ($\lambda=1$) and the engine
187 speed at around 3500 RPM.

188 Table 3. Experimental operating conditions.

Engine loads	<u>Light load</u> (23% throttle opening) <u>Medium load</u> (34% throttle opening)
Engine speed (RPM)	3500
Spark timing (CAD bTDC)	<u>Light load</u> : 28 30, 32 and 34

	<u>Medium Load:</u> 20, 24, 26 and 28
DI ratio	<u>Light load:</u> 50% <u>Medium load:</u> 56%
PI timing	410 CAD bTDC
DI timing (CAD bTDC)	<u>Early DI timing:</u> 240, 270, 300 and 330 <u>Late DI timing:</u> 60, 80, 100 and 120

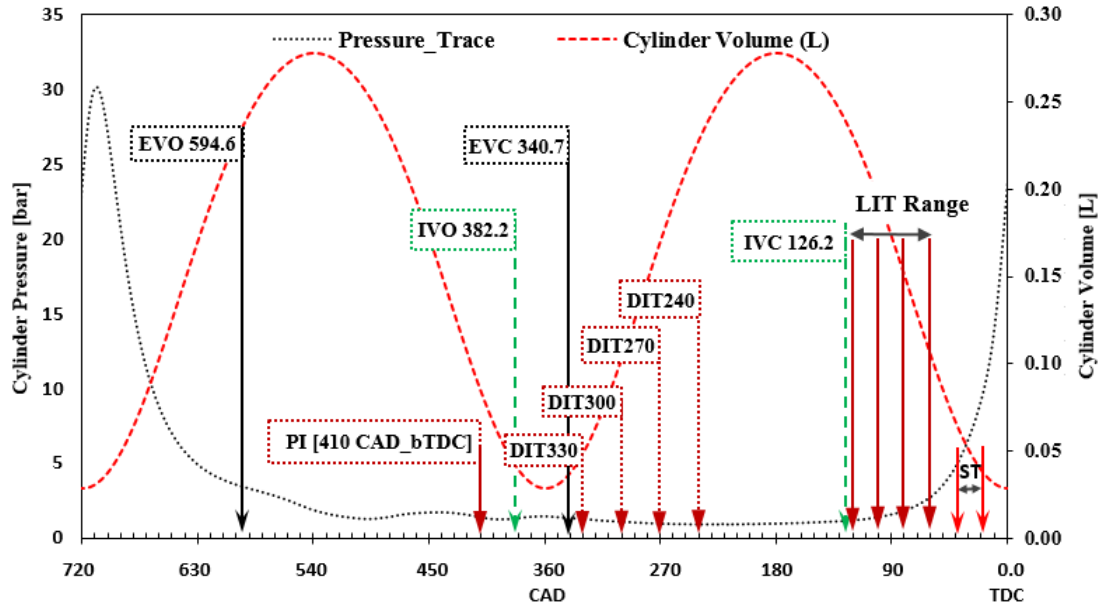


Figure 2. Valve, spark and injection timings set in the experiments.

189
190

191 A LabVIEW code was home-developed to record the engine performance and emission data.
192 Five samples were recorded at a sampling rate of 1 Hz. The average values were used in the
193 calculations and analyses. The in-cylinder pressure data was recorded at 0.5 crank angle
194 degree resolution with 100 consecutive cycles in each sample. The ensemble average of the
195 in-cylinder pressure was used to calculate the IMEP, combustion duration and heat release
196 rate. The maximum standard deviations of the emissions measurements were 6.8% for ISCO,
197 7.1% for ISNO and 3.7% for ISHC, which showed an acceptable quality of the experimental
198 data. The uncertainties of the emission measurements of the Horiba exhaust gas analyser was
199 particularised by the manufacturer in reference [38]. They are 10 ppmvol for HC, 25 ppmvol
200 for NO, 0.04 %vol for CO₂ and 0.03 %vol for CO.

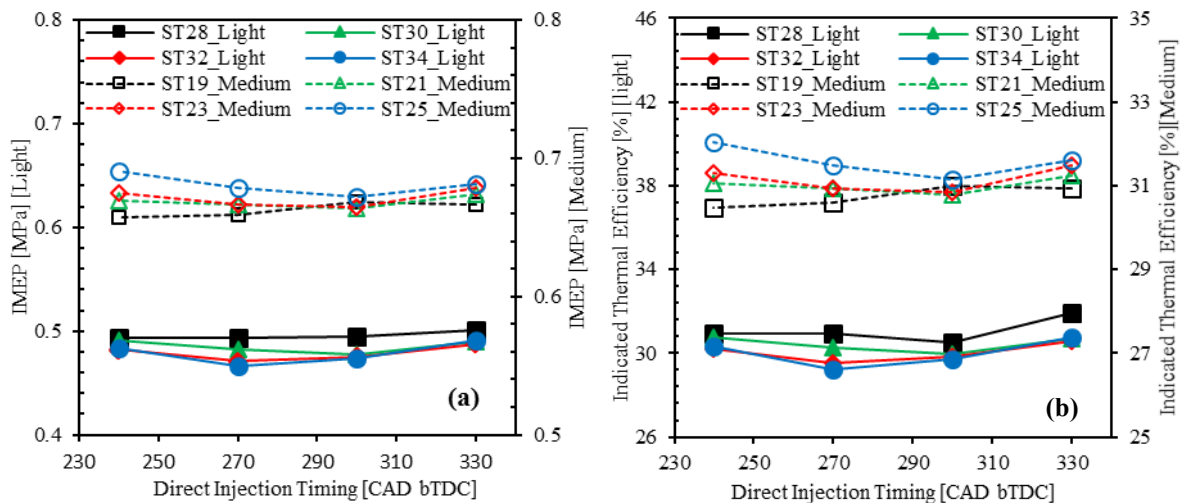
201 3 Results and Discussion

202 The experimental results will be presented and discussed as follows. Section 3.1 reports the
203 effect of early DI timing associated with spark timing on the IMEP and indicated the thermal

204 efficiency of DualEI engine. The combustion characteristics will be analysed and discussed
 205 to understand the mechanism behind the change in engine performance. In Section 3.2, the
 206 effect of early DI timing on emissions will be discussed and analysed. Sections 3.3 and 3.4
 207 will discuss the effect of late DI timing on engine performance, combustion, and emissions.

208 3.1 Effect of Early DI timing on engine performance

209 The effect of early DI timing on IMEP and thermal efficiency of DualEI engine at different
 210 spark timing is shown in Figure 3. The coefficient of variation of IMEP (COV_{IMEP}) at various
 211 DI and spark timings is shown in Figure 4. COV_{IMEP} is derived from in-cylinder pressure and
 212 measures the combustion stability (cyclic variability) [27]. As shown in Figure 4, the
 213 COV_{IMEP} is almost independent of DI and spark timings' effects at both engine loads. At light
 214 load, COV_{IMEP} remains below its maximum of 4.46% at DIT300 and ST34. At medium load,
 215 the COV_{IMEP} approaches its minimum value of 1.99% at DIT330 and ST25. The results of
 216 COV_{IMEP} shown in Figure 4 exhibit an acceptable combustion stability (less than 5%) in the
 217 full range of DI and spark timings.



218 Figure 3. Variation of IMEP (a) and indicated thermal efficiency (b) with early DI at different spark timing.

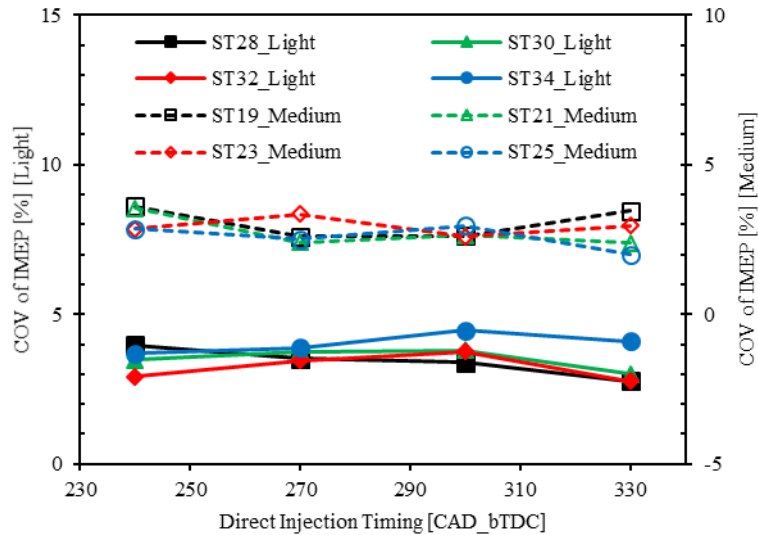


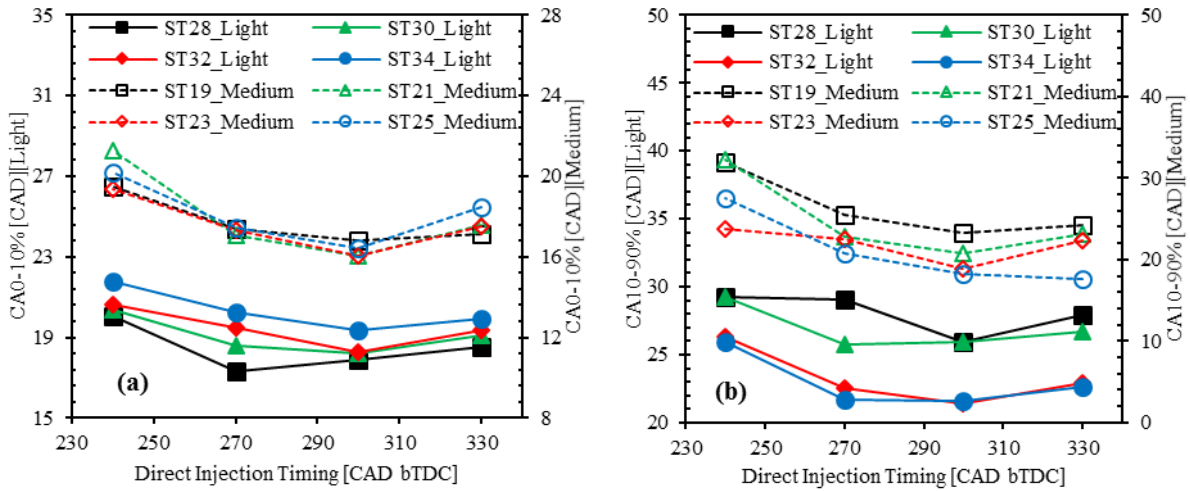
Figure 4. Variation of COV_{IMEP} with DI and spark timings.

219
220

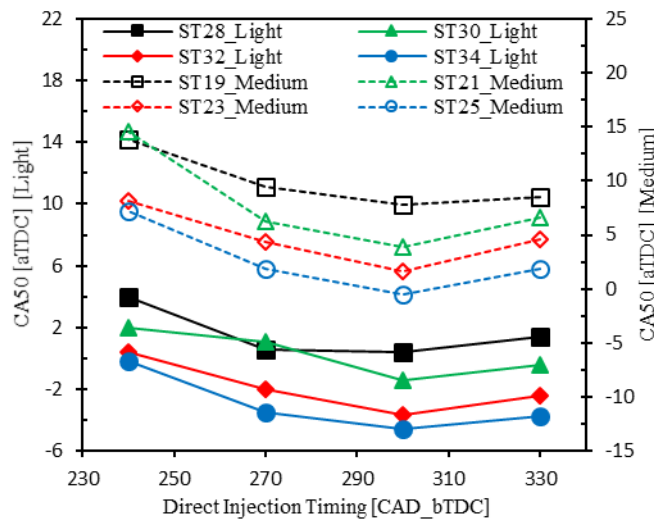
221 As shown in Figure 3, the IMEP and thermal efficiency slightly decrease when DI timing is
 222 advanced from DIT240 to DIT300 at different spark timings, except ST19 and ST28 at
 223 medium and light loads respectively. Further advancing of DI timing from DIT300 to DIT330
 224 slightly increases IMEP and thermal efficiency of DualEI engine. The reduction in IMEP and
 225 thermal efficiency might be attributed to rich air/fuel regions formed due to the impingement
 226 of ethanol that injected directly with combustion chamber walls [23] when the piston is
 227 moving upward to reduce cylinder volume, as shown in Figure 2. The increment of IMEP and
 228 thermal efficiency could be due to the longer time available at DIT330 compared with
 229 DIT300. This could potentially improve the mixing process of air with fuel before spark
 230 timing. Moreover, hot residuals might heat ethanol fuel that is directly injected at a few
 231 degrees after the exhaust valve is closed. This could increase the evaporation rate of ethanol
 232 inside the cylinder and thus improves the quality of mixture and combustion. At ST19 and
 233 ST28, IMEP and thermal efficiency increase with advanced DI timing from DIT240 to
 234 DIT330. Figure 3 shows the greatest IMEP and efficiency occur at the latest spark timing,
 235 ST19 for medium load and ST28 for a light load. The maximum increment of the IMEP
 236 occurs 1.67% at medium load and ST19, and 1.51% at light load and ST28 when the DI
 237 timing is within the range from DIT240 to DIT330.

238 To understand the combustion characteristics in DualEI engine, the results of the initial
239 (CA0-10%) and major (CA10-90%) combustion durations at different DI and spark timings
240 conditions are presented and analysed. CA0-10% is the initial combustion duration defined
241 by the crank angle degrees starting from the spark timing to the time with 10% heat release.
242 Early flame development and propagation have a strong effect on combustion stability [27].
243 As shown in Figure 5 (a), at both engine loads, CA0-10% significantly decreases with
244 advanced early DI timing from DIT240 to DIT300, and then it slightly increases when DI
245 timing is further advanced to DIT330. Spark timing shows a weak effect on CA0-10% at
246 medium load condition. However, in the light load, CA0-10% significantly decreases with
247 retarded spark timing from ST34 to ST28. The CA0-10% reduction could partially explain
248 the improved combustion stability which is shown by the COV_{IMEP} in the light load condition
249 in Figure 4. As shown in Figure 4, the COV_{IMEP} is in the range of 2%-5% when the early DI
250 timing is in the range of 240-330 CAD bTDC. It decreases from 3.5% to about 2% when the
251 spark timing is retarded from 34 to 28 CAD bTDC at DIT330. CA10-90% is the main
252 combustion duration defined by the time from 10% of the fuel burnt to 90% burnt. Figure 5
253 (b) does not show a close link between the CA10-90% and the IMEP and the indicated
254 thermal efficiency. However, CA10-90% significantly decreases when the DI timing is
255 advanced from DIT240 to DIT330 in the light load condition. Figure 6 shows the combustion
256 phase (CA50) related to the results that shown in Figure 3. CA50 is defined as the crank
257 angle degree when 50% of the fuel is burnt. As shown in Figure 6, CA50 reduces when DI
258 timing is advanced from DIT240 to DIT300 in the full set of spark timing, and at the two
259 engine loads. Then, CA50 slightly increases when DI timing is advanced further, from
260 DIT300 to DIT330. The advanced CA50 (near or even before the engine's top dead centre
261 (TDC)) means a negative indicated power could be generated. Therefore, IMEP and indicated

262 thermal efficiency slightly increase as shown in Figure 3 when CA50 decreases with
 263 advanced DI timing from 300 to 330 CAD bTDC, as shown in Figure 6.



264 Figure 5. CA0-10% and CA10-90% vs. spark timing at DIT330, light load (a) and medium load (b).

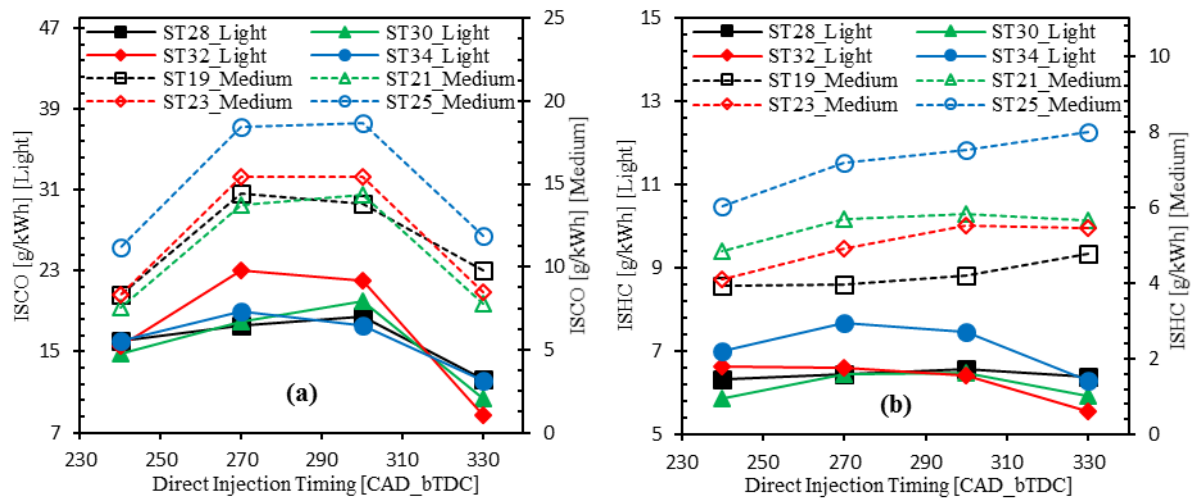


265 Figure 6. Variation of CA50 with an early DI and spark timings.

266 **3.2 Effect of Early DI timing on emissions**

267 Figure 7(a) shows the effect of early DI timing on ISCO at different spark timing. The lack of
 268 oxygen in combustion results in larger concentration of CO emission [39, 40]. As shown in
 269 Figure 7(a), the spark timing does not show a clear effect on ISCO emission when DI timing
 270 is in the range from 240 to 330 CAD bTDC. On the other hand, at both engine loads, the
 271 ISCO increases when the DI timing is advanced from DIT240 to DIT300. However, the
 272 ISCO significantly reduces when the early DI timing is further advanced to DIT330. The

273 increased CO emission could be attributed to the rich mixture regions caused by fuel
 274 impingement due to smaller combustion chamber volume with advanced DI timing, as shown
 275 in Figure 2. Sever fuel impingement could form a thick film, and slow down the fuel
 276 vaporization [41]. The decreased ISCO might be because the hot residuals heated the directly
 277 injected fuel since about half of fuel was injected at 10.7 degrees after the exhaust valve
 278 closed. This could accelerate the evaporation rate of ethanol directly injected into the cylinder
 279 [41-43]. Compared to DIT240, ISCO is increased by 85.9% at DI timings of DIT300 and
 280 2.3% at DIT330, at ST23 and medium load. At light load condition and ST32, ISCO
 281 increases by 41% when DI timing is advanced from DIT240 to DIT300, but it decreases by
 282 about 43% with advanced DI timing to 330 CAD bTDC, as shown in Figure 7 (a). The ISCO
 283 results could partly explain the results of indicated thermal efficiency shown in Figure 3 (b).



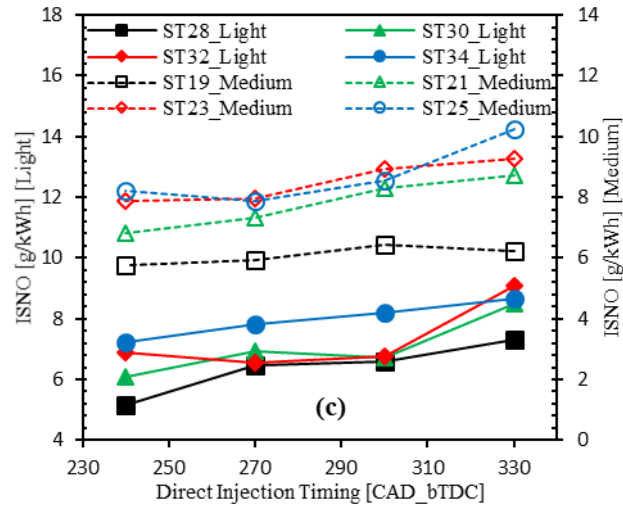


Figure 7. Variation of ISCO (a), ISHC (b) and ISNO (c) with an early DI and spark timings.

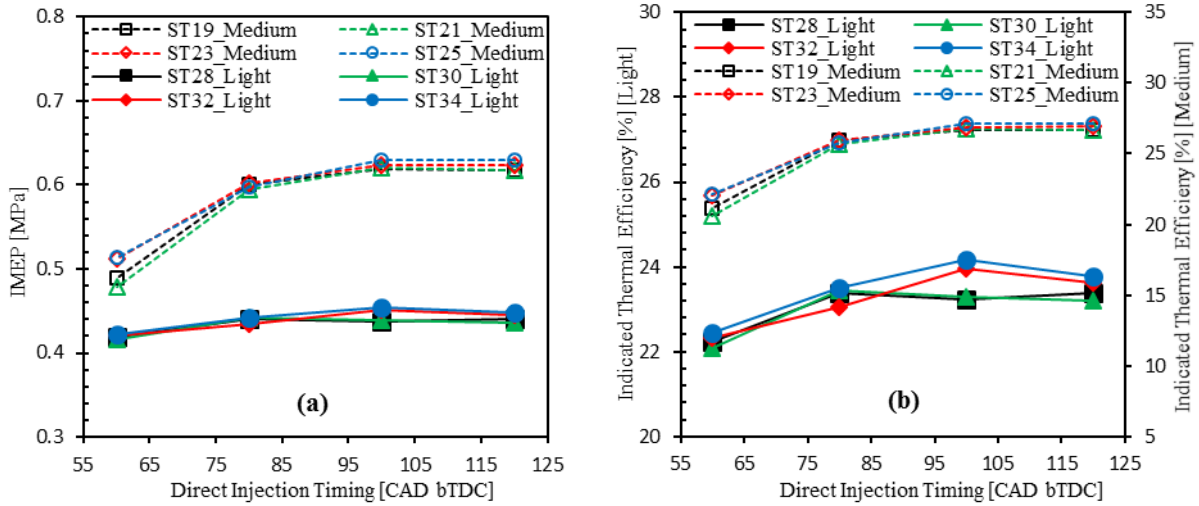
284 Figure 7 (b) shows the effect of early DI timing on HC emission at different spark timing. HC
 285 emission contains of unburned fuel from incomplete combustion due to local flame extinction
 286 that occurs when temperatures are lower and reaction times may become larger than mixing
 287 times [39, 40]. As shown in Figure 7 (b), at light load, ISHC increases when the early DI
 288 timing is advanced from DIT240 to DIT300, and then slightly decreases when DI timing is
 289 further advanced to DIT330. At medium condition, ISHC increases with advanced DI timing
 290 from 240 to 330 CAD bTDC. Spark timing exhibits a clear effect on ISHC emission that
 291 increases with advanced spark timing from ST28 to ST34 in light load, and from ST19 to
 292 ST25 in medium load. The effect of DI and spark timing is stronger in medium load than that
 293 in light load condition. Since the engine speed is fixed, the available time for the mixing
 294 process is constant for both engine load conditions. Nevertheless, the mass of fuel injected
 295 per cycle is about 45% greater (from 420 J/cycle for the light load to 610 J/cycle for the
 296 medium load) when the load increases from light to medium. This probably causes
 297 insufficient time available for forming a homogenous mixture at medium load compare to
 298 that in light load resulting in greater HC emission at the medium load condition.
 299
 300 The combination of nitric oxide (NO) and nitrogen dioxide (NO₂) forms the nitrogen oxides
 301 (NO_x) emissions which are one of the major pollutants produced by combustion [44]. In this
 302 study, only NO is measured. NO emission is formed from the N₂ and O₂ dissociation at the

303 high combustion temperature [45]. Figure 7 (c) shows that the ISNO increases with advanced
304 spark and DI timings in the light and medium load conditions. As shown in Figure 7 (c), at
305 ST21, the ISNO increases by 28% when DI timing is advanced from 240 to 330 CAD bTDC
306 in medium load. At light load and ST30, it increases by 39% when DI timing is advanced. At
307 medium load and DIT330, the ISNO increase by about 64% when the spark timing is
308 advanced from ST19 to ST25. Likewise, at light load condition but with less significant, the
309 ISNO increases when the spark timing is advanced 28 to 34 CAD bTDC.

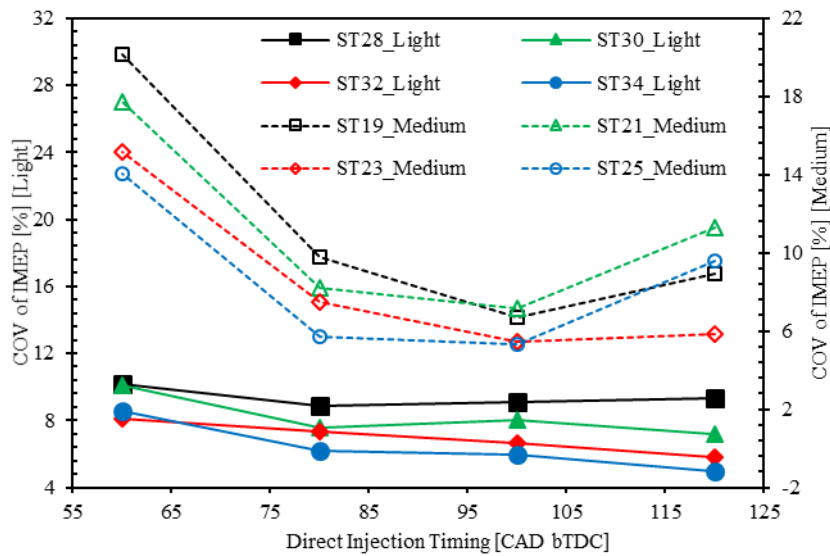
310 **3.3 Effect of late DI timing on engine performance**

311 Figure 8 shows the effect of late DI timing on the IMEP and indicated the thermal efficiency
312 of the DualEI engine at different spark timing. As shown in Figure 8, the IMEP and indicated
313 thermal efficiency are almost independent of the spark timing effect. This may be because the
314 mixture quality and condition are similar before the spark timing at each DI timing condition.
315 As shown in Figure 8, the effect of DI timing on IMEP and indicated thermal efficiency is not
316 strong in the light engine load condition. At medium load, the effect of DI timing is not so
317 obvious until the DI timing is later than 80 CAD bTDC. The IMEP slowly decreases from
318 0.62 MPa to 0.6 MPa and indicated thermal efficiency from 26.6% to 25.9% when the DI
319 timing is retarded from 120 to 80 CAD bTDC at ST19. However, the IMEP decreases from
320 0.6 MPa to about 0.5 MPa and the indicated thermal efficiency from 25.9% to about 21%
321 when the DI timing is retarded from 80 CAD bTDC to 60 CAD bTDC in the medium load
322 condition. As the engine speed is fixed at 3500 rpm, the time for mixture formation is equal
323 in light and medium load conditions. In light engine condition, 50% of the fuel is injected
324 directly in the cylinder. The time for forming the mixture of fuel and air looks sufficient as
325 the IMEP and thermal efficiency are quite stable in the full range of DI timing, as shown in
326 Figure 8. However, when the engine load is increased from light to medium condition, the
327 ratio (56%) of ethanol fuel directly injected in cylinder and the fuel flow rate are increased.

328 When the DI timing is retarded from 80 to 60 CAD bTDC, the time for the fuel to evaporate
 329 and to mix with the fuel port injected and air may become insufficient at medium load,
 330 resulting in a significant decrease in IMEP and indicated thermal efficiency.



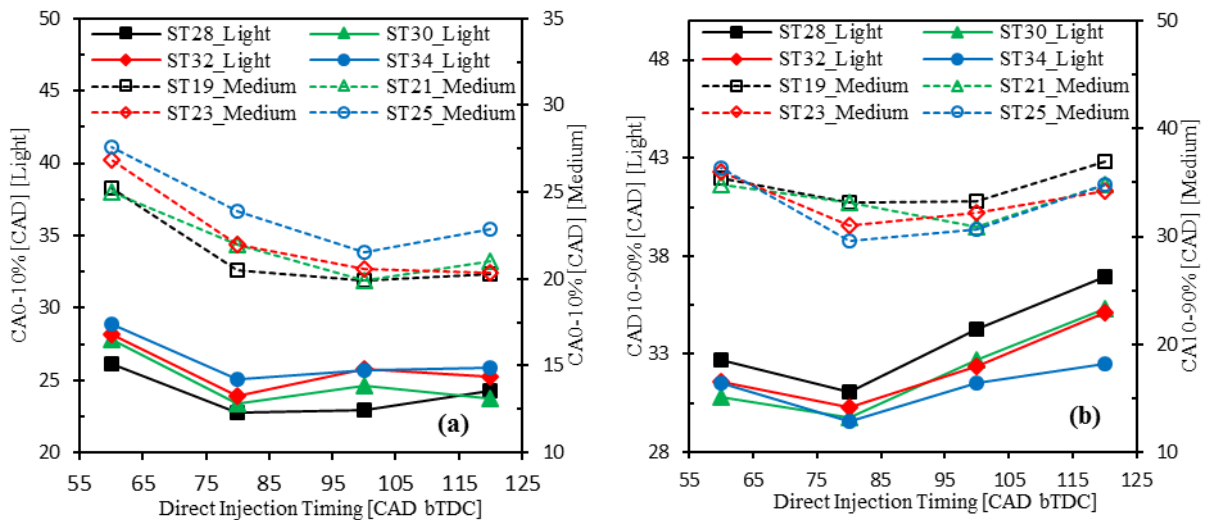
331 Figure 8. Variation of IMEP (a) and indicated thermal efficiency (b) with the late DI and spark timings.



332
 333 Figure 9. Variation of the COVIMEP with late DI and spark timing.

334 To further understand the effect of late DI timing on the engine performance, the combustion
 335 characteristics will be analyzed and discussed. Figure 10 shows the CA0-10% and CA10-
 336 90% which are corresponding to the results shown in Figure 8. Variation of IMEP (a) and
 337 indicated thermal efficiency (b) with the late DI and spark timings.. CA0-10% is the initial
 338 combustion duration defined by the crank angle degrees starting from the spark timing to the
 339 time with 10% heat release. Early flame development and propagation have a strong effect on

340 combustion stability [27]. As shown in Figure 10 (a), the effect of late DI timing on CA0-10% is not significant in the light load condition. However, in medium load condition, the CA0-10% is reduced with the DI timing advanced from 60 to 100 CAD bTDC and then slightly increased with DI timing further advanced to 120 CAD bTDC. It reduces more quickly when the DI timing is advanced from 60 to 80 CAD bTDC. The reduced CA0-10% means increased laminar flame speed and improved stability. This explains the strong effect of DI timing on the IMEP and indicated thermal efficiency when the DI timing is advanced from 60 to 80 CAD bTDC and then weak effect of DI timing with further advance of DI timing, as shown in Figure 8. Variation of IMEP (a) and indicated thermal efficiency (b) with the late DI and spark timings.. The improved combustion stability associated with reduced CA0-10% is also shown by the COV_{IMEP} in medium load condition in Figure 9. As shown in Figure 9, the COV_{IMEP} is in the range of 5%-20% when the DI timing is 60 CAD bTDC. It is decreased from 17.7% to 8.2% when the DI timing is advanced from 60 to 80 CAD bTDC at ST21. CA10-90 is the main combustion duration defined by the time from 10% of the fuel burnt to 90% burnt. Figure 10 (b) does not show a close link between the CA10-90% and the IMEP and the indicated thermal efficiency but a significant increase of CA10-90% when the DI timing is advanced from 80 to 120 CAD bTDC in the light load condition.



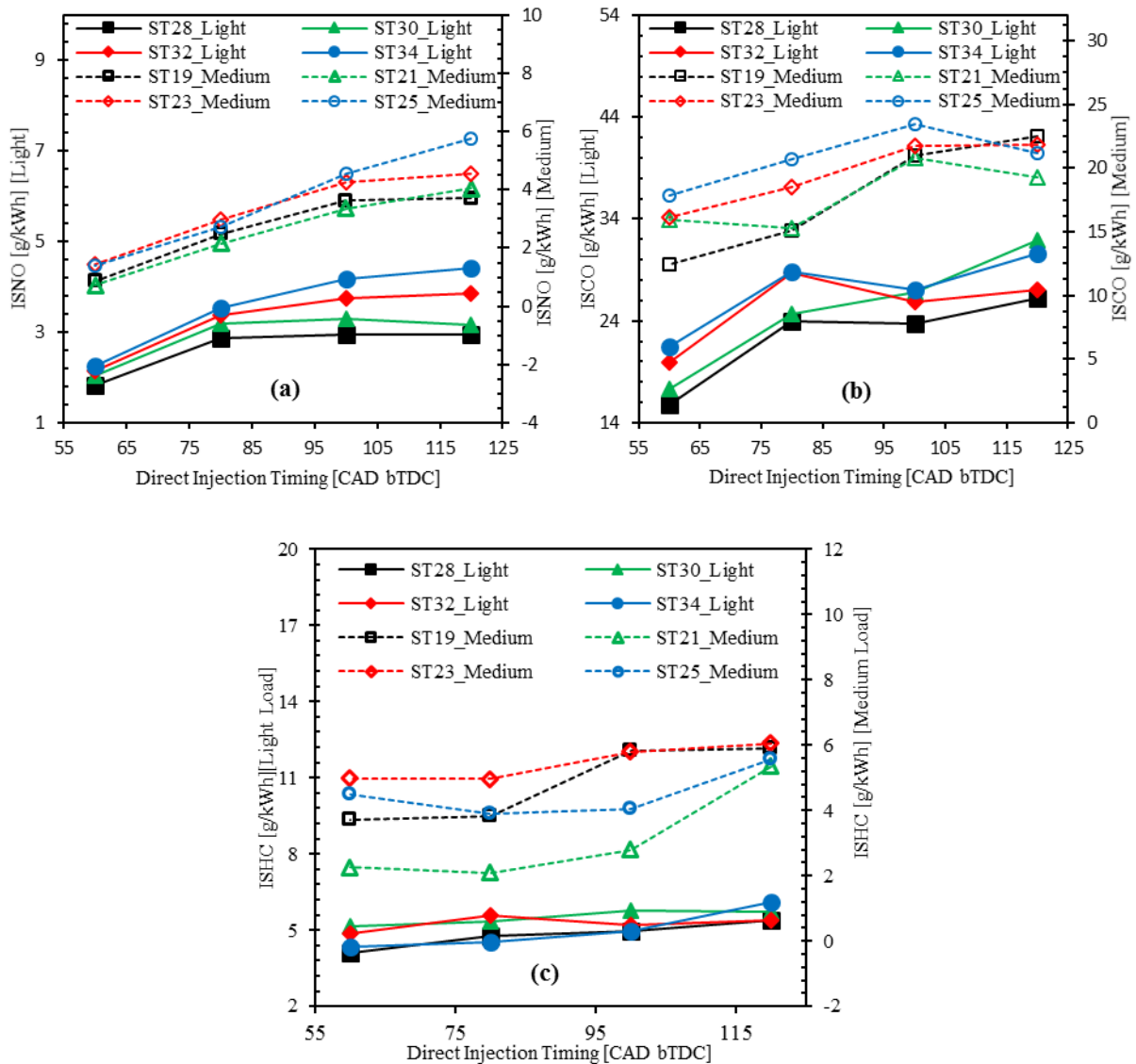
357 Figure 10. Variation of CA0-10% (a) and CA10-90% (b) with the late DI and spark timings.

358 3.4 Effect of late DI timing on emissions

359 The variation of the ISNO, ISCO, and ISHC with the DI and spark timings are presented in
360 Figure 11. Fundamentally, the elevated temperature of combustion promotes NO formation.
361 As shown in Figure 11 (a), the ISNO decreases noticeably when the late DI timing is retarded
362 from 120 to 60 CAD bTDC. It is also decreased when spark timing is retarded from ST25 to
363 ST19 in the medium load and from ST34 to ST28 in the light load condition. The cooling
364 effect of DI strategy could play a significant role in the reduction of NO emission in the late
365 DI timing condition. Advanced DI timing could reduce the mixture temperature at an earlier
366 time, but this also increases the convective heat transfer from combustion chamber walls to
367 the mixture. This could enhance the mixture quality and improve the engine performance, as
368 shown in Figure 8 and Figure 10. When the DI timing is retarded, the cooling effect due to
369 fuel evaporation associated with DI strategy could be well preserved. This could decrease the
370 combustion temperature and then the NO emission, as shown in Figure 11 (a). Figure 11 (a)
371 shows that the ISNO decreases with retarded spark timing in the light and medium load
372 conditions. This could be attributed to the smaller gas temperature due to the phase change of
373 combustion when spark timing is retarded [37].

374 The effect of DI and spark timings on ISCO and ISHC are shown in Figure 11 (b). It can be
375 seen that at all the tested spark timings, ISCO increases when the DI timing is advanced from
376 DIT60 to DIT120. Although the DIT120 provides more time for fuel evaporating compared
377 to DIT60, the in-cylinder pressure and then the temperature is lower than that of DIT60, as
378 shown in Figure 2. Greater compression temperature may promote a faster evaporation rate of
379 ethanol. Furthermore, the air/fuel equivalence ratio (λ) is slightly decreased when the DI
380 timing is advanced from DIT60 to DIT120. Consequently, less amount of oxygen is available
381 to the fixed amount of injected fuel per cycle, which result in greater ISCO and ISHC

382 emission. The ISCO and ISHC results do not show a clear link with IMEP or the results of
 383 the combustion characteristics, which are shown in Figure 8 and Figure 10.



384 Figure 11. Variation of ISNO (a), ISCO (b) and ISHC (c) with the late DI and spark timings.

385 4 Conclusions

386 Experiments were carried out to investigate the effect of DI timing associated with the spark
 387 timing on the performance of a naturally aspirated SI engine equipped with a DualEI system.
 388 The DI timing was advanced from DIT240 to DIT330 (before the intake valve is closed, early
 389 DI timing) and from DIT60 to DIT120 (after the intake valve is closed, late DI timing). At

390 each DI timing, the spark timing was varied from ST28 to ST34 at light load and from ST19
391 to ST25 at medium load. The results of this study can be concluded as follows.

- 392 1. In early DI timing conditions, the effect of DI timing on IMEP is not strong, so is that of
393 the spark timing. At medium engine load, the IMEP slightly decreases when the DI timing
394 is advanced from 240 to 300 CAD bTDC with small differences caused by the spark
395 timing. When the DI timing is further advanced from 300 to 330 CAD bTDC, the IMEP
396 increases slightly or keeps constant. At light load, the IMEP increases slightly with the
397 advanced spark timing but independently with the DI timing. As the intake valve is still
398 open in early DI timing, the mixing process and the quality of the mixture are not
399 significantly affected by the DI timing.
- 400 2. In late DI timing conditions, IMEP increases with the advanced DI timing. However, the
401 effect of DI timing is not very strong when the DI timing is earlier than 80 CAD bTDC.
402 When the DI timing is retarded from 80 to 60 CAD bTDC, the IMEP is decreased from
403 about 0.6 MPa to 0.5 MPa. This is mainly because the DI timing of 60 CAD bTDC is too
404 late and leaves insufficient time for the ethanol fuel to evaporate and mix with the air in
405 the cylinder before it is ignited. This is evident with the longer initial combustion duration
406 with DI timing of 60 CAD bTDC than that with more advanced DI timing. The ISNO and
407 ISCO increase with the advanced DI timing as well as spark timing.
- 408 3. This DualEI engine performs better with early DI timing than with late DI timing, in terms
409 of IMEP and indicated thermal efficiency. With early DI timing, the IMEP is in ranges of
410 0.60-0.68 and 0.47-0.50 MPa and indicated thermal efficiency is in ranges of 30-32% and
411 at 29-31% medium and light loads, respectively. With late DI timing, the IMEP is in a
412 ranges of 0.47-0.62 and 0.41-0.44 MPa and indicated thermal efficiency is in ranges of 21-
413 27% and 22-24% at medium and light loads, respectively.

414 **5 Acknowledgment**

415 The scholarship provided by the Iraqi Ministry of Higher Education & Scientific Research is
416 gratefully appreciated.

417 **6 References**

- 418 [1] EUR-Lex Regulation (EC) No 715/2007, 2007.
- 419 [2] Bajpai, P. *Advances in Bioethanol*. 2013 ed., Springer New Delhi Heidelberg New York
420 Dordrecht London, India, 2013.
- 421 [3] Masum, B.M., et al. Effect of ethanol–gasoline blend on NO_x emission in SI engine. *Renew.*
422 *Sustain. Energy Rev.* 2013;24:209-222, <https://doi.org/10.1016/j.rser.2013.03.046>.
- 423 [4] Reitz, R.D. Directions in internal combustion engine research. *Combust. Flame* 2013;160:1-8,
424 <https://doi.org/10.1016/j.combustflame.2012.11.002>.
- 425 [5] Huang, Y., Hong, G.,Huang, R. Numerical investigation to the dual-fuel spray combustion process
426 in an ethanol direct injection plus gasoline port injection (EDI+GPI) engine. *Energy Convers. Manag.*
427 2015;92:275-286, <http://dx.doi.org/10.1016/j.enconman.2014.12.064>.
- 428 [6] Jiao, Q.,Reitz, R.D. The Effect of Operating Parameters on Soot Emissions in GDI Engines. *SAE*
429 *Int. J. Engines* 2015;8:1322-1333, <http://doi.org/10.4271/2015-01-1071>.
- 430 [7] Montanaro, A., Malaguti, S.,Alfuso, S. Wall Impingement Process of a Multi-Hole GDI Spray:
431 Experimental and Numerical Investigation. *SAE Technical Paper* 2012-01-1266; 2012.
- 432 [8] Wang, C., et al. Impact of fuel and injection system on particle emissions from a GDI engine.
433 *Appl. Energy* 2014;132:178-191, <http://dx.doi.org/10.1016/j.apenergy.2014.06.012>.
- 434 [9] Turner, D., et al. Combustion performance of bio-ethanol at various blend ratios in a gasoline
435 direct injection engine. *Fuel* 2011;90:1999-2006, <https://doi.org/10.1016/j.fuel.2010.12.025>.
- 436 [10] Bielaczyc, P., Szczotka, A.,Woodburn, J. The Effect of Various Petrol-Ethanol Blends on
437 Exhaust Emissions and Fuel Consumption of an Unmodified Light-Duty SI Vehicle. *SAE Technical*
438 *Paper SAE Technical Paper* 2011-24-0177; 2011.

- 439 [11] Boretta, A. Analysis of Design of Pure Ethanol Engines. SAE Technical Paper SAE Technical
440 Paper 2010-01-1453; 2010.
- 441 [12] Costa, R.C., Sodr , J.R. Hydrous ethanol vs. gasoline-ethanol blend: Engine performance and
442 emissions. Fuel 2010;89:287-293, <http://dx.doi.org/10.1016/j.fuel.2009.06.017>.
- 443 [13] Robert A. Stein, C.J.H.a.T.G.L. Optimal Use of E85 in a Turbocharged Direct Injection Engine.
444 SAE Int. J. Engines 2009;2:670-682, <https://doi.org/10.4271/2009-01-1490>.
- 445 [14] Koç, M., et al. The effects of ethanol–unleaded gasoline blends on engine performance and
446 exhaust emissions in a spark-ignition engine. Renewable Energy 2009;34:2101-2106,
447 <http://dx.doi.org/10.1016/j.renene.2009.01.018>.
- 448 [15] Sjöberg, M., et al. Combined Effects of Multi-Pulse Transient Plasma Ignition and Intake
449 Heating on Lean Limits of Well-Mixed E85 DISI Engine Operation. SAE Int. J. Engines
450 2014;7:1781-1801, <http://dx.doi.org/10.4271/2014-01-2615>.
- 451 [16] Aleiferis, P., et al. Mechanisms of spray formation and combustion from a multi-hole injector
452 with E85 and gasoline. Combust. Flame 2010;157:735-756,
453 <http://dx.doi.org/10.1016/j.combustflame.2009.12.019>.
- 454 [17] Kumar, S., Singh, N., Prasad, R. Anhydrous ethanol: A renewable source of energy. Renew.
455 Sustain. Energy Rev. 2010;14:1830-1844, <http://dx.doi.org/10.1016/j.rser.2010.03.015>.
- 456 [18] Huang, Y., et al. Spray and evaporation characteristics of ethanol and gasoline direct injection in
457 non-evaporating, transition and flash-boiling conditions. Energy Convers. Manag. 2016;108:68-77,
458 <https://doi.org/10.1016/j.enconman.2015.10.081>.
- 459 [19] Engler-Pinto, C.M., de Nadai, L. Volumetric Efficiency and Air-Fuel Ratio Analysis For Flex
460 Fuel Engines. SAE Technical Paper SAE Technical Paper 2008-36-0223; 2008.
- 461 [20] Nakata, K., et al. The Effect of Ethanol Fuel on a Spark Ignition Engine. SAE Technical Paper
462 SAE Technical Paper 2006-01-3380; 2006.
- 463 [21] Taniguchi, S., Yoshida, K., Tsukasaki, Y. Feasibility Study of Ethanol Applications to A Direct
464 Injection Gasoline Engine. SAE Technical Paper SAE Technical Paper 2007-01-2037; 2007.

- 465 [22] Al-Muhsen, N.F.O., Wang, J.,Hong, G. Investigation to Combustion and Emission
466 Characteristics of the Dual Ethanol Injection Spark Ignition Engine. 20th Australasian Fluid
467 Mechanics Conference; 2016.
- 468 [23] Huang, Y., Hong, G.,Huang, R. Investigation to charge cooling effect and combustion
469 characteristics of ethanol direct injection in a gasoline port injection engine. Appl. Energy
470 2015;160:244-254, <http://dx.doi.org/10.1016/j.apenergy.2015.09.059>.
- 471 [24] Zhuang, Y.,Hong, G. Effects of direct injection timing of ethanol fuel on engine knock and lean
472 burn in a port injection gasoline engine. Fuel 2014;135:27-37,
473 <http://dx.doi.org/10.1016/j.fuel.2014.06.028>.
- 474 [25] Zhuang, Y.,Hong, G. Primary investigation to leveraging effect of using ethanol fuel on reducing
475 gasoline fuel consumption. Fuel 2013;105:425-431, <http://dx.doi.org/10.1016/j.fuel.2012.09.013>.
- 476 [26] Zhu, G., Hung, D.,Schock, H. Combustion characteristics of a single-cylinder spark ignition
477 gasoline and ethanol dual-fuelled engine. Proceedings of the Institution of Mechanical Engineers, Part
478 D: Journal of Automobile Engineering 2010;224:387-403, [DOI: 10.1243/09544070JAUTO1236](https://doi.org/10.1243/09544070JAUTO1236).
- 479 [27] Heywood, J.B. Internal Combustion Engine Fundamentals. McGraw-Hill, Inc., 1988.
- 480 [28] Hakansson, A. CA50 estimation on HCCI engine using engine speed variations. Lund
481 University: MSc Thesis, 2007.
- 482 [29] Ayala, F.A., Gerty, M.D.,Heywood, J.B. Effects of Combustion Phasing, Relative Air-fuel Ratio,
483 Compression Ratio, and Load on SI Engine Efficiency. SAE Technical Paper SAE Technical Paper
484 2006-01-0229; 2006.
- 485 [30] de O. Carvalho, L., de Melo, T.C.C.,de Azevedo Cruz Neto, R.M. Investigation on the Fuel and
486 Engine Parameters that Affect the Half Mass Fraction Burned (CA50) Optimum Crank Angle. SAE
487 Technical Paper 2012-36-0498; 2012.
- 488 [31] Zoldak, P.,Naber, J. Spark Ignited Direct Injection Natural Gas Combustion in a Heavy Duty
489 Single Cylinder Test Engine - Start of Injection and Spark Timing Effects. SAE Technical Paper SAE
490 Technical Paper 2015-01-2813; 2015.

491 [32] Jo, Y., Bromberg, L., Heywood, J. Optimal Use of Ethanol in Dual Fuel Applications: Effects of
492 Engine Downsizing, Spark Retard, and Compression Ratio on Fuel Economy. SAE Int. J. Engines
493 9(2) 2016;9:1087-1101, <http://dx.doi.org/10.4271/2016-01-0786>.

494 [33] Jo, Y., Bromberg, L., Heywood, J. Octane Requirement of a Turbocharged Spark Ignition Engine
495 in Various Driving Cycles. SAE Technical Paper 2016-01-0831; 2016.

496 [34] Davy, M.H., Williams, P.A., Anderson, R.W. Effects of Injection Timing on Liquid-Phase Fuel
497 Distributions in a Centrally-Injected Four-Valve Direct-Injection Spark-Ignition Engine. SAE
498 Technical Paper 982699; 1998.

499 [35] Huang, Y., et al. The Effect of Fuel Temperature on the Ethanol Direct Injection Spray
500 Characteristics of a Multi-hole Injector. SAE Int. J. Fuels Lubr. 2014;7:792-802,
501 <http://dx.doi.org/10.4271/2014-01-2734>.

502 [36] Motorsport, B. HP Injection Valve HDEV 5.2. 2017.

503 [37] Al-Muhsen, N.F.O., Hong, G. Effect of Spark Timing on Performance and Emissions of a Small
504 Spark Ignition Engine with Dual Ethanol Fuel Injection. SAE Technical Paper 2017-01-2230; 2017.

505 [38] HORIBA Ltd. MEXA-584L Automotive Emission Analyzer Manual. HORIBA, Ltd., 2007.

506 [39] Dunn-Rankin, D., Therkelsen, P. Lean Combustion - Technology and Control (2nd Edition).
507 Elsevier.

508 [40] Tiechman, G.P.M.C.S.R. Combustion Engine Development Mixture Formation, Combustion,
509 Emissions and Simulation. 2012.

510 [41] Schulz, F., et al. Gasoline Wall Films and Spray/Wall Interaction Analyzed by Infrared
511 Thermography. SAE Int. J. Engines 2014;7:1165-1177, <http://dx.doi.org/10.4271/2014-01-1446>.

512 [42] Kar, K., et al. Measurement of Vapor Pressures and Enthalpies of Vaporization of Gasoline and
513 Ethanol Blends and Their Effects on Mixture Preparation in an SI Engine. SAE International Journal
514 of Fuels and Lubricants 2008;1:132-144, 10.4271/2008-01-0317.

515 [43] Yaws, C.L. Yaws' Handbook of thermodynamic and physical properties of chemical compounds
516 : physical, thermodynamic and transport properties for 5,000 organic chemical compounds. Knovel,
517 USA, 2003.

- 518 [44] Huang, Y., et al. Tackling nitric oxide emissions from dominant diesel vehicle models using on-
519 road remote sensing technology. Environmental Pollution 2018;243:1177-1185,
520 <https://doi.org/10.1016/j.envpol.2018.09.088>.
- 521 [45] Gonca, G. Influences of different fuel kinds and engine design parameters on the performance
522 characteristics and NO formation of a spark ignition (SI) engine. Applied Thermal Engineering
523 2017;127:194-202, <https://doi.org/10.1016/j.applthermaleng.2017.08.002>.